CHAPTER II
BACKGROUND AND LITERATURE SURVEY

2.1 Background

2.1.1 Two-Phase Flow

For a vertical pipe with two-phase flow, there are four main regimes, as shown in Figure 2.1 and Figure 2.2, occurring successively at ever-increasing gas flow rates:

(a) *Bubble flow*: There is a continuous liquid phase and the gas phase is dispersed as bubbles within the liquid continuum. The bubbles travel with a complex motion, causing some of the bubbles to coalesce and generally be of non-uniform sizes.

(b) *Slug flow*: This flow pattern, in vertical systems, is sometimes referred to as plug flow, and occurs when the bubble size becomes comparable to that of the channel diameter, and characteristic bullet-shaped bubbles are formed. A bubble surrounded by a thin liquid film is often called a Taylor bubble. The liquid between the Taylor bubbles often contains a dispersion of smaller bubbles.

(c) *Churn flow*: At higher gas velocities, the Taylor bubbles in slug flow break down into an unstable pattern in which there is a churning or oscillatory motion of liquid. This flow occurs more predominantly in wide-bore tubes and may not be so important in narrow-bore tubes where the region of churn flow is small.

(d) *Annular flow*: This configuration is characterized by liquid traveling as a film on the channel walls, with gas flowing through the center. Part of the liquid can form as droplets dispersed in the central gas core.

(e) *Mist flow*: The velocity of the continuous gas phase is so high that it reaches as far as the tube wall and entrains the liquid in the form of droplets.

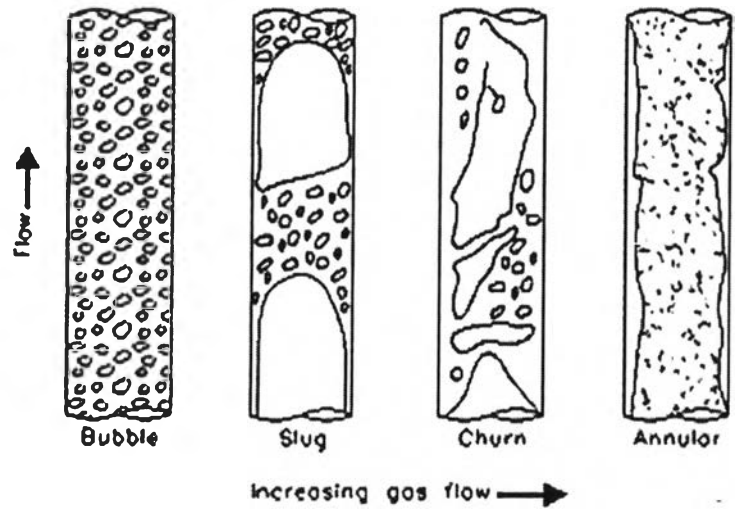

Figure 2.1 Modeling flow pattern transitions for a steady upward gas-liquid flow in vertical tubes (Bornea and Dukler, 1980).

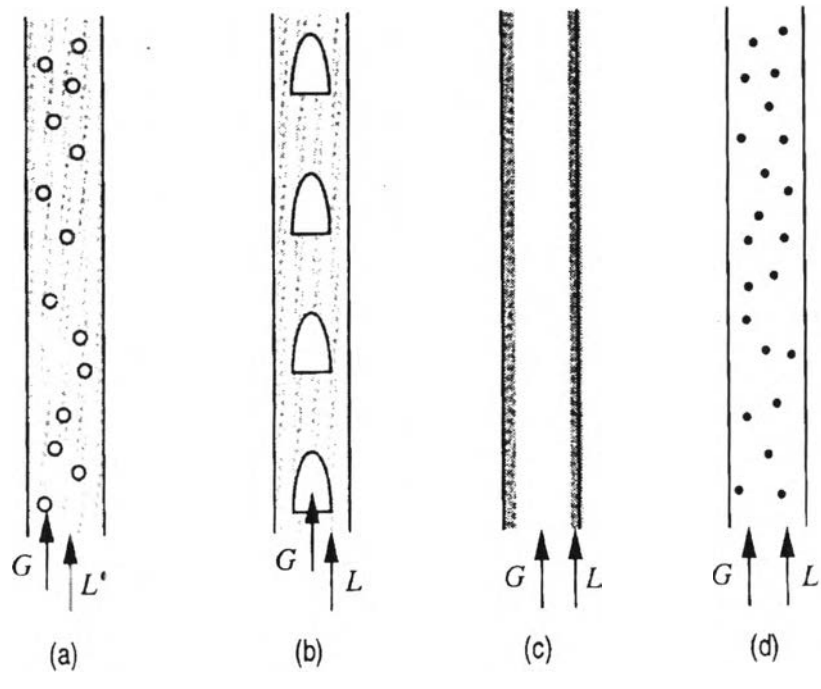

Figure 2.2 Two-phase flow regimes in a vertical tube: a) the bubble flow ; b) the slug flow; c) the annular flow ; and d) the mist flow. In each case, the gas is shown in white, and the liquid is shaded in black (Wilkes, 1999).

2.1.2 Determination of Flow Regime

A typical situation occurs when the gas and liquid volumetric flow rates G and L are specified, and the pressure gradients, (dp/dz), and void fractions, ε, [Nicklin,1961] are calculated. Correlations for these last two variables are more likely to be successful if we know or recognize a flow regime and develop relationships specifically for it. The following approximate demarcations are recognized:

1. *Bubble/slug flow transition.* Small bubbles introduced at the base of a column of liquid will usually eventually coalesce into slugs. The transition depends very much on the size of the bubbles, how they were introduced, the distance from the inlet, and on surface tension effects, so there is no simple criterion for the transition.

2. Slug/annular flow transition. In the narrow gap between the gas and the tube wall at the base of the slugs, there is a significant downwards flow of liquids, and hence a fairly strong relative velocity between gas and liquid at this point. With increasing gas flow rates, this results in an instability of the liquid film, which can start bridging the whole cross section of the tube. These bridges can in turn be broken up by the gas and the flow becomes chaotic.

3. *Annular/mist flow transition.* The transition is ill defined because most annular flow entrains some droplets.

2.1.2.1 Bubble Flow Pattern

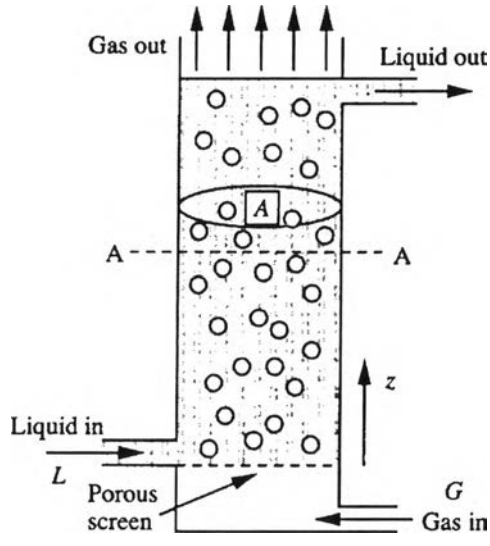

Figure 2.3 Bubble flow (Wilkes, 1999).

Gas bubbles and liquid in upward co-current flow are shown in Figure 2.3. The mean upward liquid velocity across plane A-A is

$$\bar{u}_l = \frac{Q_G + Q_L}{A} \tag{1}$$

where Q_G = volumetric flow-rate of gas, l/min, Q_L = volumetric flow-rate of liquid, l/min, A = cross-sectional area of a tube, m^2 The rise velocity of gas bubbles below plane A-A is relative to that of a moving liquid which has a velocity, $\bar{u}_l$, the mean upward liquid velocity that across plane A-A in figure 2.3. So that velocity of the gas bubbles is:

$$v_g = \bar{u}_l + u_b = \frac{Q_G + Q_L}{A} \tag{2}$$

where u_b is the bubble velocity rising into a stagnant liquid and the total volumetric flow rate of gas is

$$Q_G = \varepsilon A v_g \tag{3}$$

The void fraction is given by

$$\frac{Q_G}{\varepsilon A} = \frac{Q_G + Q_L}{A} + u_b \qquad \text{or} \qquad \varepsilon = \frac{Q_G}{Q_G + Q_L + u_b A} \tag{4}$$

u_b = bubble rise velocity (m/s) Bubble rise velocity, u_b rising into a stagnant liquid was proposed by Peebles and Garber [1953] from the equations in Table 2.1:

Table 2.1 Terminal velocities for bubble

Region	*Range of Applicability*	*Terminal Velocity, u_b*
1	$\mathrm{Re}_b \leq 2$	$\frac{2R_b^2(\rho_l - \rho_g)g}{9\mu_l}$
2	$2 < \mathrm{Re}_b \leq 4.02G_1^{-0.214}$	$0.33g^{0.76}\left(\frac{\rho_l}{\mu_l}\right)^{0.52} R_b^{1.28}$
3	$4.02G_1^{-0.214} < \mathrm{Re}_b \leq 3.10G_1^{-0.25}$	$1.35\left(\frac{\sigma}{\rho_l R_b}\right)^{0.5}$
4	$3.10G_1^{-0.25} < \mathrm{Re}_b$	$1.53\left(\frac{\sigma g}{\rho_l}\right)^{0.25}$
5	$R_b \geq 2.3\sqrt{\frac{\sigma}{g\rho_l}}$	$1.00\sqrt{gR_b}$
	In the above: $\mathrm{Re}_b = \frac{2\rho_l u_b R_b}{\mu_l}$,	$G_1 = \frac{g\mu_l^4}{\rho_l \sigma^3}$,

where g = gravitational acceleration constant (m/s^2), and R_b = radius of the sphere having the same volume as the bubble, and is half the equivalent diameter, D_e (m).

Predicting pressure gradients in the upwards vertical direction, we may note that the density of the liquid, which occupies a fraction (1-ε) [occupied by the liquid] of the total volume, is much greater than that of the gas. For relatively low liquid velocities, it is likely to be encountered in the bubble flow regime, the friction factor term is negligible. Therefore, the pressure gradient consists only the hydrostatic effect:

$$\left(-\frac{dp}{dz}\right) = \rho_L\, g\, (1 - \varepsilon) \tag{5}$$

2.1.2.2 Slug Flow Pattern

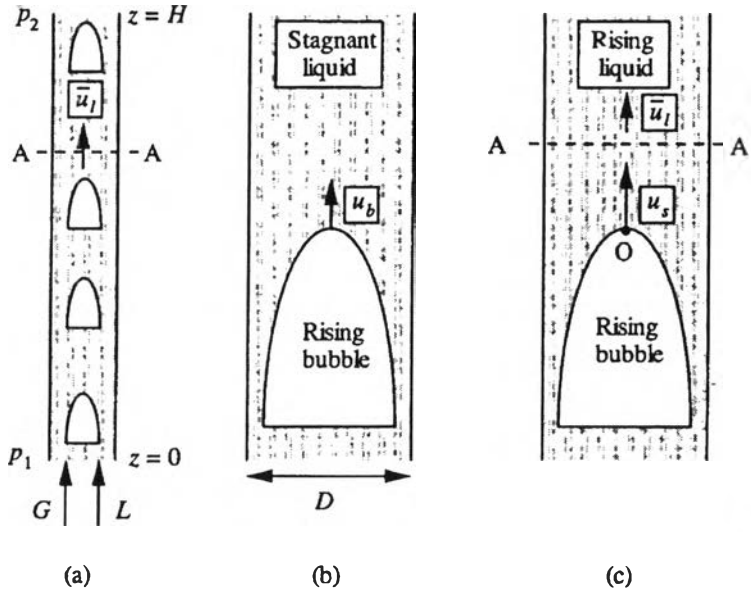

Figure 2.4 Two-phase slug flow in a vertical pipe: (a) ascending gas and liquid, (b) rising bubble in stagnant liquid; (c) rising bubble in moving liquid (Wilkes, 1999).

Figure 2.4 (a) shows the gas and liquid flow upwards together at single volumetric flow rates Q_G and Q_L, in a pipe of internal diameter D. An upward liquid velocity (u_l) across a plane A-A is ahead of a gas slug. The total upward volumetric flow rate of liquid across A-A must be the combined gas and liquid flow rate which enters at the bottom. Therefore the mean liquid velocity at plane A-A is $\bar{u}_l = (Q_G+Q_L)/A$, in which A is the cross-sectional area of the pipe.

Figure 2.4 (b) shows a different situation, in which a single bubble is moving steadily upward with a rise velocity u_b in a stagnant liquid. Davies and Taylor (1950) used an approximate analytical solution for the non-viscous liquid such as water and light oils, which is

$$u_b = c\sqrt{g\,D} \tag{6}$$

where the constant, c, is 0.33, and g is the gravitational acceleration. From the experimental data, the constant "c" was experimentally found to be equal to 0.35.

The slug rises in a stagnant liquid as shown in Figure 2.4 (b), but the mean velocity of liquid is the highest velocity at the center of the pipe-near the nose of the slug. Nicklin, Wilkes, and Davidson (1962), showed the value of liquid velocity of to be about 1.2 time of the mean liquid velocity near the "nose" O of the slug, 1.2 $\bar{u}_l$, when the Reynolds numbers was greater than 8,000.

Hence, the true rise velocity of the slug is:

$$u_s = 1.2\frac{Q_G + Q_L}{A} + u_b = 1.2\frac{Q_G + Q_L}{A} + 0.35\sqrt{gD} \tag{7}$$

For the conservation of the gas; this gives:

$$Q_G = U_s A\varepsilon \tag{8}$$

Substituting u_s in equation (8) into equation (7)

$$\frac{Q_G}{\varepsilon A} = 1.2\left(\frac{Q_G + Q_L}{A}\right) + 0.35\sqrt{gD} \quad \text{or} \quad \varepsilon = \frac{Q_G}{1.2(Q_G + Q_L) + 0.35\sqrt{gD}} \tag{9}$$

Equation (9) can be solved for the void fraction when the gas and liquid flow rates are known.

Predicting the pressure gradient for slug flow, the wall friction of the liquid "piston" between successive gas slugs will be of secondary importance and we need to consider the equation (10). So, the single-phase frictional pressure gradient for liquid only, flowing at a mean velocity, $\bar{u}_l$, is a more accurate for the pressure gradient in slug flow regime. The expression for the pressure gradient for the slug flow is:

$$\left(-\frac{dp}{dz}\right) = (1-\varepsilon)\left[\rho_L g + \left(\frac{dp}{dz}\right)_{sp}\right] \tag{10}$$

The single-phase frictional pressure gradient for the liquid only is:

$$\left(-\frac{dp}{dz}\right)_{sp} = \frac{2 f_F \rho_L \overline{u_L}^2}{D} \tag{11}$$

2.1.2.3 Churn or Froth Flow Pattern

The froth flow pattern has been variously called the churn, the froth, the wave entrainment, the dispersed plug, and the semi-annular flows. It is similar to the slug pattern in that the flow that is pulsating and there are alternate slugs of gas and liquid. At the higher flow rates, characteristics of froth flow are the bubble wakes, which become more agitated, a large number of small bubbles are torn off at the tail, and the whole wake becomes richer in bubbles. The froth pattern differs from the regular orderly slug flow pattern in that neither the bubbles of gas nor the slug of liquid maintain their identity as they moved up the tube.

The pattern occurs over a modest range of superficial gas velocities and apparently only up to a certain critical superficial liquid velocity. It is a transition pattern from the regular slug flow to the annular and the mist flow. At any given liquid rate, the pattern extends from the point of breakdown of the regular liquid slugs and gas bubbles to a gas velocity sufficient to carry the bulk of the liquid up the wall of the tube by the surface drag exerted.

The froth flow pattern is not amenable to theoretical analysis and has not been the subject of any extensive experimental study.

2.1.2.4 Annular-Mist Flow Pattern

The annular-mist flow pattern is widely encountered in the flow of gas-liquid mixtures at high gas rates and gas-liquid ratios. The annular-mist flow pattern in gas-liquid systems is characterized by an upward moving, continuous, and smooth-to-wavy film of liquid on the tube wall and a much more rapidly moving central core of gas, containing entrained droplets of liquid in a concentration which may vary from low to high. The liquid film may be totally in laminar motion or it may be laminar only in the vicinity of the wall, and turbulent close to the gas-liquid interface.

Shearer and Nedderman, (1965) divided the annular-mist flow pattern into the "small ripple" regime and the "disturbance wave" regime. In the small ripple regime, small waves develop on the liquid surface and move at velocities of the order of the interface velocities and then lose their identity. At higher liquid flow rates, the waves are larger, and they travel at velocities two to five times the interfacial velocity. These waves are known as disturbance waves.

At any given liquid flow-rate, decreasing the gas rate causes more of the liquid to be present in the film, the liquid film velocity to decrease, and its thickness to increase. At a certain critical gas flow-rate the liquid film velocity becomes zero, and below this rate the liquid film thickness increases rapidly, and it has a negative velocity near the wall. The liquid film penetrates the gas phase at the center, and the froth flow occurs. As the gas rate is increased, turbulence takes place in the liquid film, the thickness of the film decreases, waves develop at the interface, and increasing number of droplets are torn from the film and entrained in the gas. Eventually the continuous film is destroyed and almost all the liquid is transported as entrained droplets in the gas phase.

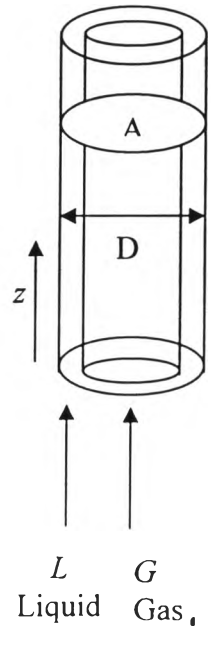

Figure 2.5 Vertical annular two-phase flow (Wilkes, 1999).

Consider the simultaneous flow of gas and liquid in a vertical tube in Figure 2.5. First, consider just the flow of gas in the inner core. Since the gas velocity v_g is typically much higher than that of the liquid, the pressure gradient may be approximated as if the gas were flowing with velocity v_g in a pipe of diameter D_g, giving:

$$\left(\frac{dp}{dz}\right)_{tp} = \left(\frac{dp}{dz}\right)_{g} = -\frac{2f_F\ \rho_g\ v_g^2}{D_g} - \rho_g g = \phi_g^2 \left(\frac{dp}{dz}\right)_{go} - \rho_g g \qquad (12)$$

Second, consider the entire flow, obtaining the frictional contribution from the viewpoint of the liquid:

$$\left(\frac{dp}{dz}\right)_{tp} = \phi_l^2 \left(\frac{dp}{dz}\right)_{lo} - \left[\varepsilon\ \rho_g + (1-\varepsilon)\ \rho_l\right] g \qquad (13)$$

For specified gas and liquid flow rates, the derivatives on the right-hand sides of both equations will be determined by calculations. These equations can then be solved simultaneously for the two-phase flow pressure gradient $(dp/dz)_{tp}$ and the void friction ε.

2.2 Literature Survey

2.2.1 Two-Phase Flow

The study carried out by Davies and Taylor (1950) can be divided into two parts. Part I describes measurements of the shape and the rising rate of air bubbles of various volumes between 1.5 to 200 cm^3 when they rise through nitrobenzene or water. Measurements of photographs of bubbles formed in nitrobenzene show that the greater part of the upper surface is always spherical. A theoretical discussion is based on the assumption that the pressure over the front of the bubbles is the same as that in ideal hydrodynamic flow round a sphere. The rise velocity, U, should be related to the radius of curvature, R, in the region of the vertex, by the equation $U = (2/3)\sqrt{g\,R}$; the agreement between this relationship and the experimental results is excellent. For geometrically similar bubbles of such large diameter that the drag coefficient would be independent of Reynolds number, it would be expected that U would be proportional to the sixth root of the volume, V; measurements of eighty-eight bubbles show considerable scatter in the values of $U/V^{1/6}$, although there is no systematic variation in the value of this ratio with the volume.

Part II reveals that though the characteristics of a large bubble are associated with the observed fact that the hydrodynamic pressure on the front of a spherical cap moving through a fluid is nearly the same as that on a complete sphere, the mechanics of a rising bubble cannot be completely understood if the observed pressure distribution on a spherical cap is understood. Failing this can cause the case of a large bubble running up a circular tube filled with water and emptying at the bottom, which is capable of being analyzed completely, since the bubble is not then followed by a wake. An approximate calculation shows that the rise velocity U is U = $0.46\sqrt{ga}$, where "a" is the radius of the tube. Experiments with a tube diameter of 7.9 cm gave values of U from 29.1 to 30.6 cm/sec, corresponding with values of U/ $\sqrt{ga}$ from 0.466 to 0.490.

Govier, Radford, and Dunn (1957) distinguished six different flow patterns: bubble, slug, froth or churn, annular and mist each occurring at successively higher air rates. Table 2.2 and Figure 2.6 summarize in scale drawings and a tabulated form of the results of photographic observations of the flow patterns observed at low, medium, and high water rates, and over a range of air rates. Govier (1957) also presented pressure gradient data of each flow regimes in Figure 2.7. He defined pressure drops regimes I, II, III, and IV by the loci line such that regime I extends to gas flow rates defined by the first pressure drop minimum, regime II from the first pressure drop minimum to the pressure drop maximum, regime III from the pressure drop maximum to the second minimum, and regime IV beyond the second minimum. The loci lines in the total pressure gradient curve are related to change in the flow patterns as illustrated in figure. These relations enabled to support their visual observations of flow pattern changes with the more quantitative detection of the pressure gradient minimum and maximum points.

Wallis (1969) has mentioned flow-pattern boundaries for a vertical upwards flow of air and water in Figure 2.8, previously presented by numerous authors. Hall-Taylor and Hewitt ((1962) presented various regimes or subdivisions of the annular flow pattern for a cocurrent upward flow of air and water in Figure 2.9.

Table 2.2 Flow pattern details for air-water mixture flowing in 1.025 inch I.D vertical pipe (see Figure 2.8)

Sketch Identification	Flow Pattern	Continuous Phase	Superficial Velocity		Volume Fraction Oil, E_o	Holdup Ratio, H	Slip Velocity, S ft/sec
			Water, V_{SL} ft/sec	Oil, V_{SO} ft/sec			
A	bubble	water	0.1	0.015	0.08	1.70	0.08
B	bubble	water	0.1	0.058	0.17	2.85	0.22
C	slug	water	0.1	0.167	0.32	3.60	0.38
D	froth	neither	0.1	0.562	0.67	2.80	0.54
E	froth	neither	0.1	1.11	0.87	1.62	0.49
F	mist	oil	0.1	2.94	0.97	0.84	−0.58
G	mist	oil	0.1	9.0	0.99	0.72	−3.53
H	bubble	water	1.0	0.015	0.01	1.26	0.26
I	bubble	water	1.0	0.058	0.035	1.60	0.62
J	bubble	water	1.0	0.22	0.114	1.71	0.80
K	slug	water	1.0	0.49	0.24	1.52	0.69
L	froth	neither	1.0	1.61	0.58	1.17	0.40
M	froth	neither	1.0	2.0	0.65	1.10	0.28
N	mist	oil	1.0	5.0	0.85	0.92	−0.52
O	mist	oil	1.0	9.0	0.909	0.90	−1.10
P	bubble	water	10.0	0.015	0.0014	1.05	0.50
Q	bubble	water	10.0	0.058	0.005	1.10	1.00
R	bubble	water	10.0	0.22	0.02	1.10	1.02
S	bubble	water	10.0	0.49	0.04	1.10	1.04

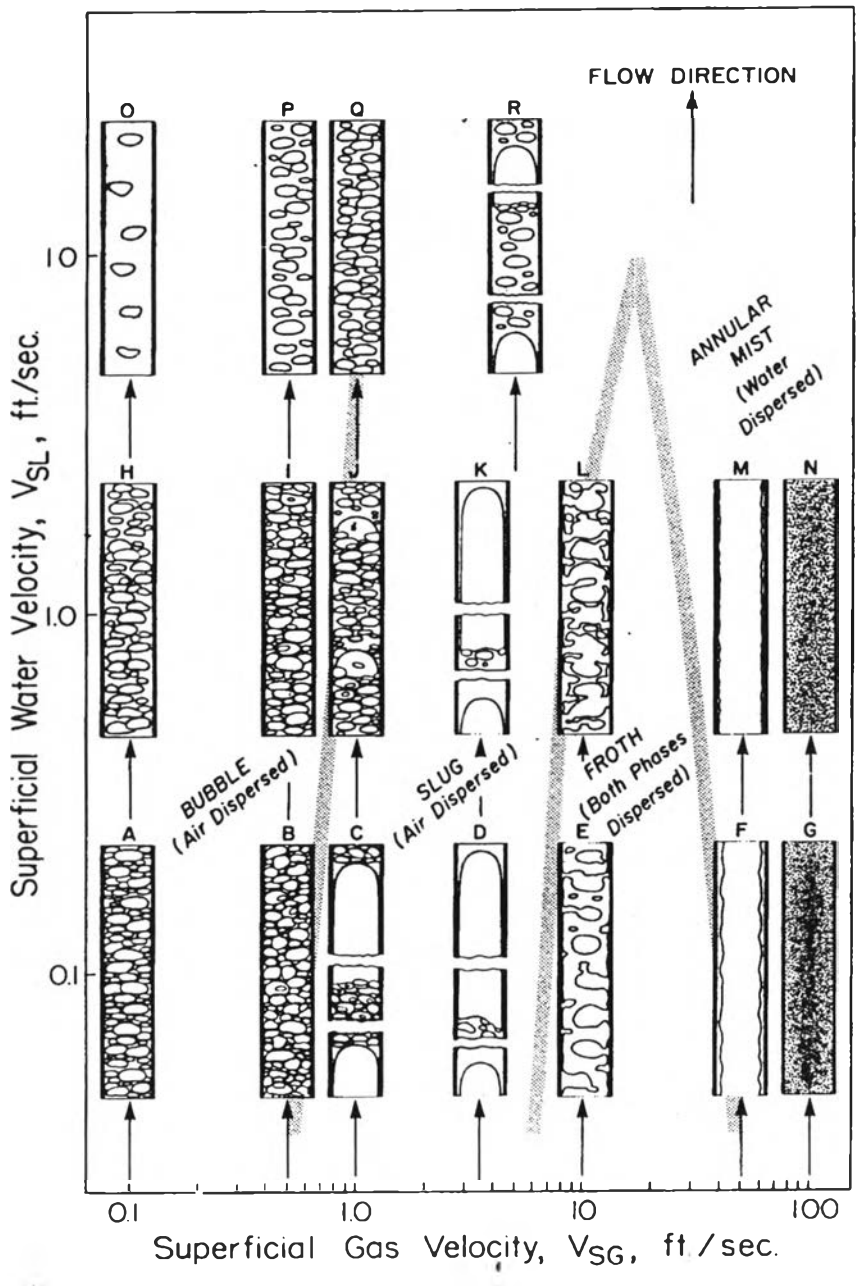

Figure 2.6 Flow pattern for air-water mixtures flowing in a 1.025- inch pipe based on observations and calculations (Govier, Radford, and Dunn, 1957).

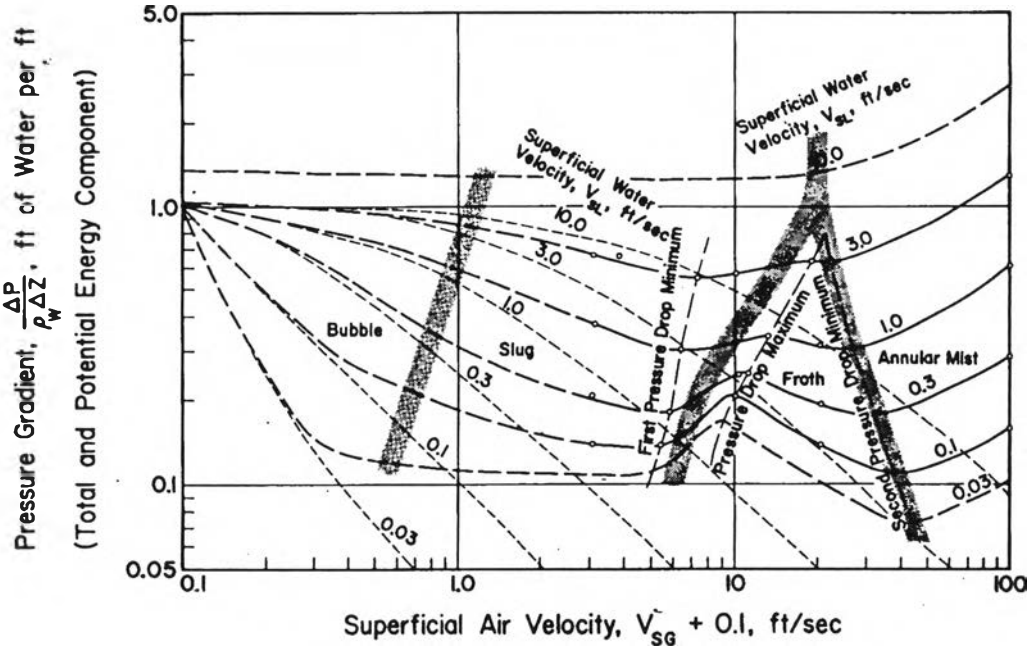

Figure 2.7 Pressure gradient data for air-water mixtures in a 1.025 inch pipe (Govier, Radford, and Dunn, 1957).

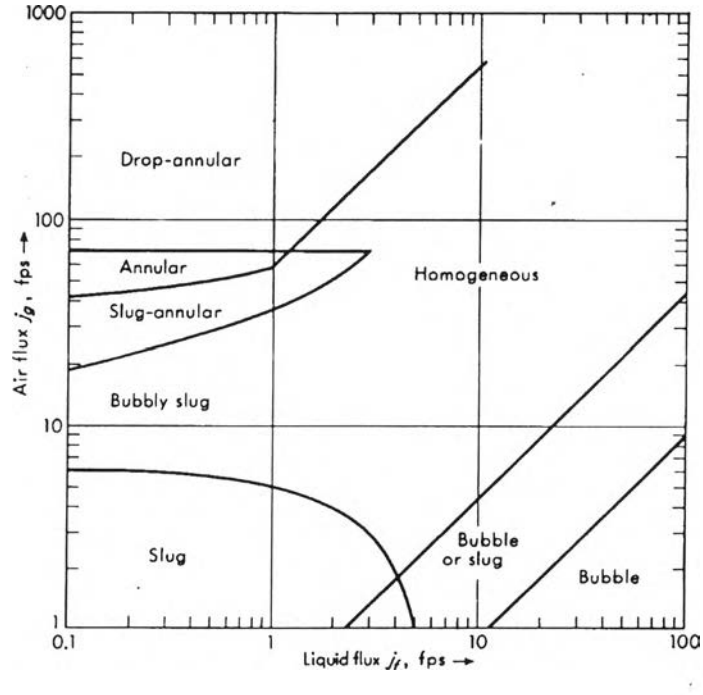

Figure 2.8 Flow-pattern boundaries for vertical upflow of air and water at 15 psia in a 1 inch diameter tube (Wallis, 1969).

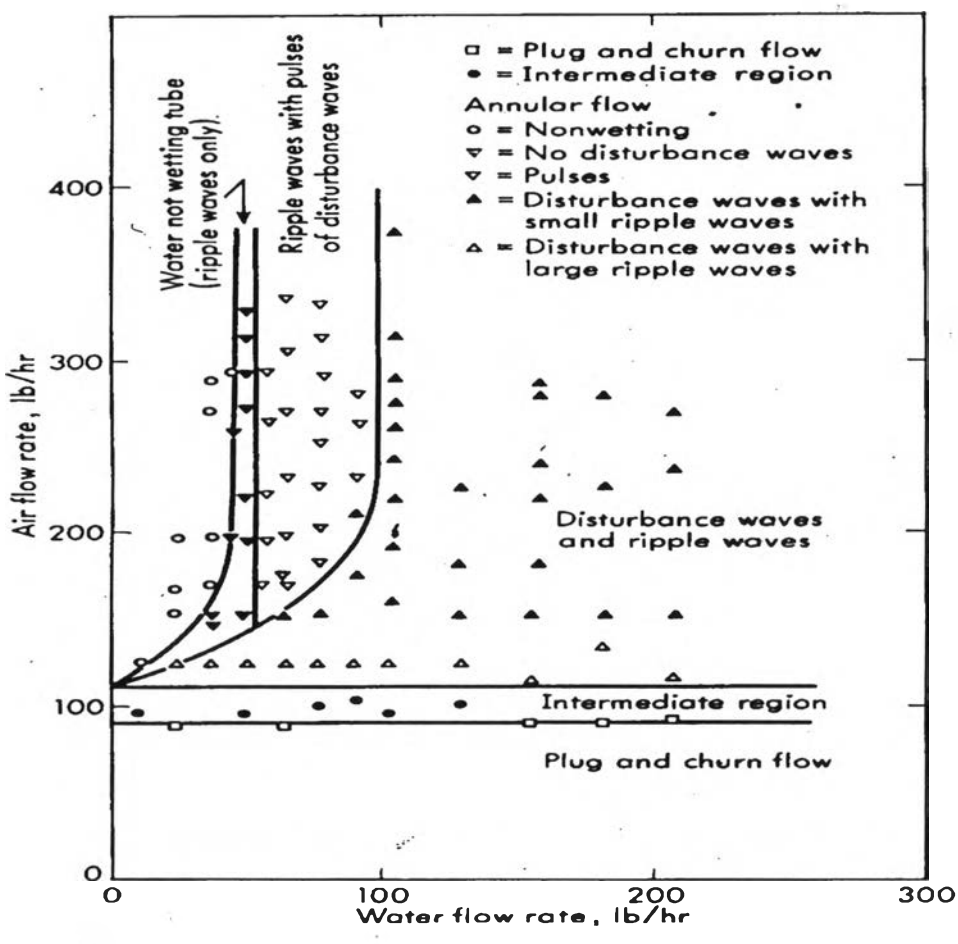

Figure 2.9 Various "regimes" or subdivisions of the annular flow pattern for cocurrent upward flow of air and water in a 1.25 inch diameter pipe at 15 psia (Hall-Taylor, and Hewitt, 1962).

Nicklin (1962) studied the properties of long bubbles in vertical tubes. It has been shown that these bubbles rise relative to the liquid ahead at a velocity exactly equal to the rising velocity of wakeless bubbles of the type studied by Dumitrescu and Taylor (1950). For 1-inch tubes, this velocity is closely predicted by motion of bubbles in moving liquid streams that have been studied, and the results applied to the problem of two-phase slug flow. An expression for the voidage in a steady two-phase slug flow has been derived, and this predicted voidage agrees well with the experimental results.

Welsh, Ghiaaisaan, and Abdel-Khalik (1999) studied experimentally in countercurrent flow limitation (flooding), two-phase flow patterns, and the void

fraction in countercurrent flow of gas-pseudoplastic liquids in a vertical and inclined channel. They found that the gas and liquid superficial velocity ranges in the experiments were 0.5-198 and 0.8-34 cm/s, respectively. The visually observed two-phase flow regimes were the bubbly-slug, the slug, the slug-churn, the churn, and the annular flows occurring only at the near-flooding conditions. The flow regime transition lines showed significant differences with data representing a Newtonian liquid with a viscosity of the same order of magnitude as the polymer solution apparent viscosities. The slug flow pattern, characterized by Taylor bubbles, was the most dominant flow pattern. The measured void fractions were correlated based on the drift flux model, using different correlation parameters for the bubbly/slug, and the slug or the slug/churn flow regimes.

Fukano and Furukawa (1998) investigated the effects of liquid viscosity on the mean liquid film thicknesses, wave heights, and gas-liquid interfacial shear stresses in the vertical-upward co-current annular flow in a 26.0 mm inner diameter tube. Water and glycerol solutions were used as working fluids to change the kinematic viscosity of liquid from 0.85×10^{-6} to 8.6×10^{-6} m^2/s. The mean liquid film thicknesses and wave heights were determined using the signals of time-varying cross-sectionally averaged holdups, which were detected by a constant-current method at a distance of about 3.5 m from an air-liquid mixer. The pressure gradients were also measured by a U-tube manometer. From their observation of the shape of waves of the liquid holdup signals, and the still photographs of gas-liquid interfaces it is clear that the interfacial structure is strongly dependent on the liquid viscosity. As liquid viscosity increases, the interfacial friction factor decreases when compared under the same mean liquid film thickness because the wave height decreases with increasing viscosity, but it increases under the same Reynolds numbers of gas phase because of density increases with increasing viscosity. In their proposed method the only information needed is the superficial gas and liquid velocities if the inner diameter of the tube and fluids properties (liquid viscosity, densities of gas and liquid) are known.

Wongwises and Kongkiatwanitch (2001) presented new data on the gas-liquid interfacial friction factor in an annular two-phase upward co-current flow in a vertical circular pipe. Their studies have been performed at relatively high film

thickness, taking into consideration the effect of the entrained droplets which occur from the break up of the disturbance waves. The entrained liquid flow rate was measured by using a sampling probe connected with a cyclone separator. The entrainment flow rate in the gas core is calculated from an assumption that the sampling is carried out in an isokinetic manner. The calculated parameters like entrainment volumetric flow rate, entraining droplets velocities and depositing droplet velocities have been included in their model was modified from the literature to determine the interfacial shear stress. The interfacial friction factor was further determined by using the relationship between the interfacial shear stress and interfacial friction factor. The changes in the air flow rate and the water film thickness have been found to have an effect on the interfacial friction factor.

Henning Arendt Knudsen and Alex Hansen (2001) studied the relation between pressure and fractional flow in two-phase flow in porous media. They studied average flow properties in porous media using a two-dimensional network simulator. It models the dynamics of two-phase immiscible bulk flow where film flow can be neglected. The boundary conditions are biperiodic, which provide a means of studying steady-state flow where complex bubble dynamics dominate the flow picture. In particular, for the case of two phases having equal viscosities, they find that the derivative of the fractional flow is related to the global pressure drop. Hopefully, after their experimental verification, they got an important equation from numerical work. So, this equation can be of use in the measurement of two- phase flow properties.